Jurnal Fizik Malaysia Volume 43 Issue 1 (2022) pgs 10139-10150 N. I. Ishak

Quantum Walk in Noisy Environment: Dynamics at the Borders of Quantum-Classical Transition

Nur Izzati Ishak[a], S. V. Muniandy[a] & W. Y. Chong[b]

[a]*Center for Theoretical and Computational Physic, Department of Physics, Faculty of Science, University of Malaya, Kuala Lumpur, 50603, Malaysia*
[b]*Photonics Research Centre, University of Malaya, Kuala Lumpur, 50603, Malaysia*

(Received: 31.7.21 ; Published: 1.7.22)

Abstract. This article provides a brief review on the generalization of quantum walk to accommodate noise. Several measures of quantumness are presented. Decoherence and disorder affect the evolution of the quantum walk, particularly the quantum speedup that is measured using the mean square displacement. This can be translated into a broad characteristic of quantum to classical transition in the form of localization phenomena.

Keywords: Quantum walk, Quantum channel, Decoherence, Disorder

I. INTRODUCTION

Quantum walk (QW) has become a popular research subject among the quantum computing and information community as it promised the way towards the scalable quantum machine. It shows superior efficiency with the quadratically faster variance and mixing time as compared to its classical counterpart. This "quantum advantage" means the performance of some of the classical-based algorithms can be made faster via quantum machine [1]. In the cyclic nodes, the quantum walker at the odd numbers of nodes does not mix to form uniform distribution, while the classical walker is always mixed into uniform distribution [2]. These dynamics of QW provide a flexible platform for the development of novel algorithms in the quantum query, element distantness, and quantum network routing [1,3,4]. Quantum walk is also used in the modelling of energy transfer in the photosynthesis process [5], fast computing the integer factorization [6], and database searching [7]. Additionally, the unique form of quantum walks class of probability density function (PDF) and small entropy can be utilized in the application of algorithm development, data compression, and cryptography [8,9].

The physical realization of quantum walk required the maintenance of a pure qubit state such that the unitary evolution of the quantum system is free from the environment interaction. The quantum state is very fragile, as it can easily lose its "quantumness" from the simple action of measurement, observation, noise, or perturbation resulting in the decohered states. From any of these actions, the quantum states can undergo the quantum to classical (Q-C) transition as the quantum properties between states are reduced. For example, measurement, noise, and disorder can cause the wave function of the quantum state to collapse into a single classical localized state. Two mechanisms of inducing the transition of the quantum states into classical states are decoherence (no energy lost into the environment) and dissipation (energy lost to the environment).

Paper contributed to the National Physics Conference 2021 (PERFIK2021), 29 – 30 June 2021

Both mechanisms resulted from the interaction of the quantum states with the environment that caused the loss of quantum information from the system to the environment [8].

The foundation of quantum computing is to build a stable coherent qubit state. Decoherence reduces the quantum correlation and quantum interferences between states, thus triggering the Q-C transition which is undesirable consequences. As it is impossible to escape from the unwanted interaction (noise), does it imply the impossibility of manipulating the quantum system? With the current progress in quantum-based hardware, the noiseless quantum operation is difficult to apply. In 2018, a noisy 50-100 qubit quantum computer was built that works on the noisy intermediate-scale quantum scheme (NISQ), and this opens up the NISQ-era technology [10]. It is shown experimentally that the QW via edge state in the dissipative non-Hermitian system exhibits endurance against the static perturbations and disorder [11]. Additionally, Brayvi et al.[12] demonstrated the possibility of gaining the quantum advantage in running the quantum algorithm through the noisy shallow quantum circuits. Hence, utilizing the noisy QW is a more realistic aim. With the realistic expectation, quantum technology now focused on utilizing noise in quantum computing and processing.

This review compares different noisy DTQW in producing Q-C transition and the measurable quantifier of this transition. In this review, we first overview the standard and noisy (decoherence) DTQW, followed by the measure of quantumness or non-classicality. We then discuss the impact of decoherence and disorder on the DTQW under different noise effects.

II. QUANTUM WALK

In the simple one-dimensional classical random walk CRW model, a walker is allowed to move either to the left or right based on the outcome of a random event, for example tossing a coin. If the outcome from tossing a coin is the head, the walker moves to the right and vice versa. By repeating the process of shifting the walker conditioned by the coin's outcome for many numbers of times, the probability of the walker covering across the position space converges to the Gaussian distribution with the linear spread of $\sigma^2 \propto t$.

On the other hand, the quantum walk moves across the Hilbert space via the quantum coin operator that allows the walker to exist in a superposition of two internal degrees of freedom simultaneously. Each application of a quantum coin without measuring the outcome of the coin will allow the walker to shift over the position space in the parallel superposition state, resulting in the farther spread of distribution with the ballistic variance as $\sigma^2 \propto t^2$. The probability distribution generated by the quantum walk shows the unique multimodal distribution with two high peaks at the ends of the lattice points covering a large distance of position space. Quantum walk can be further into three classes namely: discrete-time quantum walks (DTQW), continuous-time quantum walks (CTQW), and stochastic quantum walk (SQW). DTQW scheme operation is based on the application of the coin and shift-conditioned evolution operator in discrete steps [13], while CTQW evolves according to the Hamiltonian evolution operator [14]. SQW covers the coherence and incoherent dynamics of the non-unitary evolution of the quantum system via Lindblad master equation that includes the coherent dynamics Hamiltonian operator and incoherent term of Lindblad operator. In this review, we focus on the DTQW only.

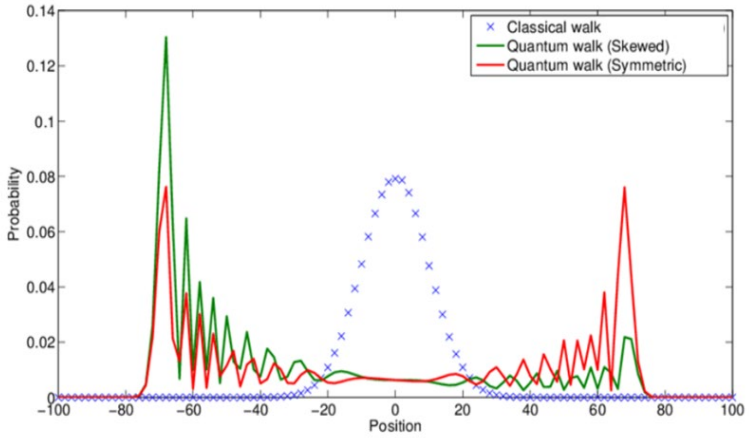

FIGURE 1. Probability distribution generated by the DTQW with skewed initial state $|\Psi_0\rangle = 1/\sqrt{2}(|0\rangle + |1\rangle)$ (green), symmetric initial state of $|\Psi_0\rangle = 1/\sqrt{2}(|0\rangle + i|1\rangle)$ (red) and CRW (blue-cross) in the position space over 200 iteration steps.

III. DISCRETE-TIME QUANTUM WALK

The numerical implementation of the discrete-time quantum walk involves applying coin and shift-conditioned evolution operator in discrete steps onto the evolving density matrix without taking any intermediate measurement. The tunable DTQW can be implemented by controlling the different types of quantum coins operator [15,16], shift operator [17], and walker's initial states [18] which regulate the feature of the quantum walk. Discrete-time quantum walk is defined in the composite Hilbert space of $\mathcal{H} = \mathcal{H}_c \otimes \mathcal{H}_x$ consisting of a two-dimensional coin Hilbert space $\mathcal{H}_c$ spanned with basis of $\{|0\rangle, |1\rangle\}$ representing the qubit's internal degree of freedom, and N dimensional position Hilbert space $\mathcal{H}_x$ spanned by basis of $|x\rangle$ representing the lattice points. General initial state of quantum walk at the origin is given by:

$$|\Psi_0\rangle = \left(\cos(\delta)|0\rangle + \mathrm{e}^{i\eta}\sin(\delta)|1\rangle\right) \otimes |x = 0\rangle, \tag{1}$$

with complex amplitude of qubit state δ and phase factor η. At each step of the walk, a single parameter quantum coin operator C parametrized by $0° \leq \theta \leq 90°$ given by:

$$C = \begin{bmatrix} \cos(\theta) & \sin(\theta) \\ \sin(\theta) & -\cos(\theta) \end{bmatrix}, \tag{2}$$

is applied on the internal degree of freedom of the qubit in the coin's Hilbert space, followed by the conditioned-shift operator S acting on position space:

$$S = |0\rangle\langle 0| \otimes \sum_{x \in Z} |x-1\rangle\langle x| + |1\rangle\langle 1| \otimes \sum_{x \in Z} |x+1\rangle\langle x|, \tag{3}$$

that resulted in the spatial entanglement between Hilbert space $\mathcal{H}_c$ and $\mathcal{H}_x$. As the result, the shifting direction of the walk will depend on the outcome of the applied quantum coin operator i.e., if the resulted internal coin state is $|0\rangle(|1\rangle)$the walker can move to left (right). Both the coin and the shift-conditional operator are expressed in the form of the unitary walk operator of:

$$W = S(C \otimes \mathbb{I}), \tag{4}$$

that govern the whole evolution of quantum walk by iterating it for t-steps of iteration without taking any intermediate measurement, then the final state of the walker given by:

$$|\Psi(t)\rangle = W_\theta^t \Psi(0) = W_\theta^t[|\psi\rangle \otimes |x=0\rangle], \quad (5)$$

with $\mathbb{I}$ as identity operator will create the superposition of all possible pathways.

The coin parameter θ controls the speed of the walk such that the variance of QW at t number of steps is shown to depend on a single parameter θ only such as by changing the value of θ, $\sigma^2(t) \approx (1 - sin\,\theta)t^2$ [15]. As different coin parameter value yields different interference pattern, one can optimize the performance of DTQW by tuning the parameter $\theta \leq 45°$. The quantumness performances measured by PDF, variance, entropy, and fidelity are enhanced with the small choice coin parameter[16, 19]. In fact, under $\theta = 0°$, a walker undergoes "quasi-classical" walk with ballistic variance without assistance from the interference mechanisms or undergoing diffusion i.e., absence of the quantumness. Without interference or diffusion, the unitary quantum walks coin is unable to fully reach the quantum-to-classical transition, which is considered as the limit of quantum walks.

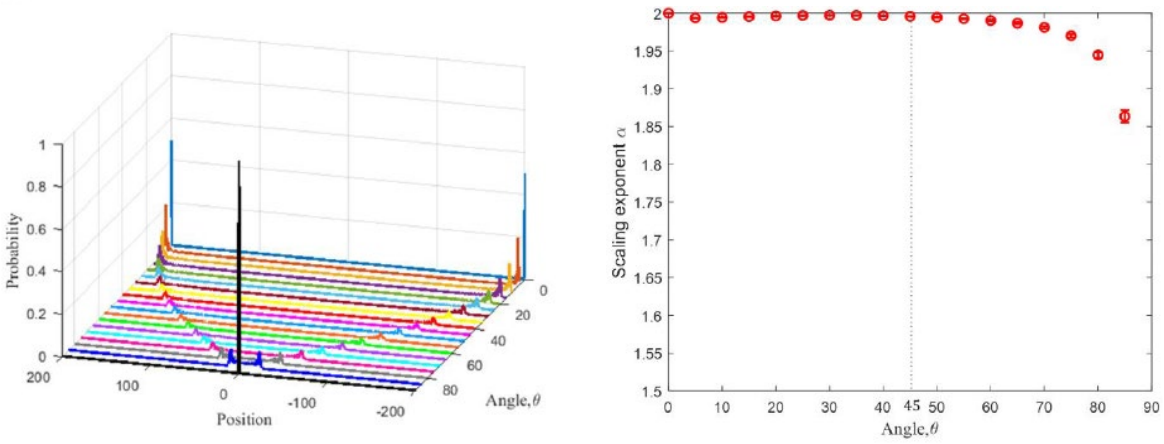

(a) (b)

FIGURE 2. (a) Probability distribution and (b) variance's scaling exponent (see Eq. (9)) of the standard DTQW with initial state of $|\Psi_0\rangle = 1/\sqrt{2}(|0\rangle + i|1\rangle)$ under variation of coin parameter $0° \leq \theta < 90°$ after 200 steps of iteration [19].

The different preparation of the walker's initial states allows the control of possible direction taken by QW in the position space. For example, the asymmetric wavefunction with the initial condition $|\Psi_0\rangle = 1/\sqrt{2}(|0\rangle \pm |1\rangle) \otimes |0\rangle$, the walk driven by Hadamard coin (fair coin) produced the asymmetric probability distribution across the position space. Similarly, varying the qubit state δ and phase factor η allows the control in the propagation of the walker in position space through the producing asymmetrical distribution. To obtain an equal possible direction taken by walk, the walker's initial state must be in a symmetric initial superposition state in form of $|\Psi_0\rangle = 1/\sqrt{2}(|0\rangle \pm i|1\rangle) \otimes |0\rangle$.

IV. NOISY CHANNEL DISCRETE-TIME QUANTUM WALKS

When the DTQW interacts with the environment, the evolution may no longer be unitary and the system is called an open system. The dynamic of the open system DTQW can be modelled using the mathematical formulation known as quantum operation [20]. Quantum operation

describes the changes of discrete state of the initial state ρ to the final state ρ' without explicit reference to time. The advantage of this formulation is one does not need the exact detail of the environment that induces the evolution of walk. Via the general map of quantum operation $\varepsilon(\rho)$ in form of Kraus operator E_k the evolution of the initial state ρ to the final state ρ' is given by:

$$\rho \to \rho' = \varepsilon(\rho) = \sum_k E_k \rho E_k^\dagger, \tag{6}$$

with the effects of environment /physical process that caused decoherence captured in the choice of the Kraus operator. The set of operators $\{E_k\}$ of Kraus operator satisfies $\sum E_k^\dagger E_k = I$ and is not necessarily unitary. The map $\varepsilon(\rho)$ is linear $\varepsilon(\alpha\rho_1 + \beta\rho_2) = \alpha\varepsilon(\rho_1) + \beta\varepsilon(\rho_2)$, trace-preserving $\mathrm{Tr}[\varepsilon(\rho)] = \mathrm{Tr}(\rho)$, completely positive (if $\rho \geq 0$, then $\varepsilon(\rho) \geq 0$), and completely positive trace preserving (CPTP). In the open DTQW scheme the Krauss operator is used to model the noise channel where it is applied together with the coined-shifted walk evolution operator Equation (4) at each step of the walk for t-steps of iterations evolution of density matrix. The common models of the noise channel used in modelling decoherence are summarized as below:

TABLE 1. Kraus operator representation of the noise channel with p_c is the probability of the qubit state being affected by the decoherence/noise level, X, Y, Z the Pauli operators, and χ a parameter related to temperature, T. For further details refer to [17,23].

Noise Channel	Krauss operator
Bit-flip channel	$E_0 = \sqrt{1-p_c}\,\mathbb{I}\ ,\ E_1 = \sqrt{p_c}X$
Phase damping channel	$E_0 = \sqrt{1-p_c}\,\mathbb{I}\ ,\ E_1 = \sqrt{p_c}Z$
Depolarizing channel	$E_0 = \sqrt{1-3p_c/4}\,\mathbb{I}\ ,\ E_1 = \sqrt{p_c/4}\,X$ $E_2 = \sqrt{p_c/4}Y\ ,\ E_3 = \sqrt{p_c/4}\,Z$
Amplitude damping channel	$E_0 = \begin{bmatrix} 1 & 0 \\ 0 & \sqrt{1-p_c} \end{bmatrix},\ E_1 = \begin{bmatrix} 1 & \sqrt{p_c} \\ 0 & 0 \end{bmatrix},$
General amplitude channel	$E_0 = \sqrt{\chi}\begin{bmatrix} 1 & 0 \\ 0 & \sqrt{1-p_c} \end{bmatrix}, E_1 = \sqrt{\chi}\begin{bmatrix} 0 & p_c \\ 0 & 0 \end{bmatrix}$ $E_2 = \sqrt{1-\chi}\begin{bmatrix} \sqrt{1-p_c} & 0 \\ 0 & 1 \end{bmatrix},\quad E_3 = \sqrt{1-\chi}\begin{bmatrix} 0 & 0 \\ \sqrt{p_c} & 0 \end{bmatrix}$

V. QUANTIFIER OF Q-C TRANSITION

There are few quantities that can be used to discuss the Q-C transition. The probability density distribution of the walker at position x and step t defined as

$$P_x(x,t) = |\langle x|\Psi(t)\rangle|^2 = |a_x(t)|^2 + |b_x(t)|^2 \tag{7}$$

where a_x and b_x are the complex amplitudes of the states. This quantity is useful to describe the spatial spread of the walker. Quantum behavior is depicted by the oscillation and maximum peak at both end sides of lattice. Next, one may consider the variance defined as

$$\sigma^2 = \sum_{\mathrm{x}=1}^{N} P_x(x-\mu)^2, \tag{8}$$

where $\mu = \sum_{x=1}^{N} P_x x$ represents the mean of the distribution with number of position sites $N = t_{\max} + 1$. The scaling behaviour of the variance with respect to the time step captures the spread dynamics as follows:

$$t^{\alpha} = \begin{cases} \alpha = 2 & \text{ballistic,} \\ 1 < \alpha < 2 & \text{superdiffusion,} \\ \alpha = 1 & \text{normal,} \\ 0 < \alpha < 1 & \text{subdiffussion.} \end{cases} \tag{9}$$

Quantum walk refers to the quadratic scaling behaviour, namely $\sigma^2 \propto t^2$ implying ballistic transport. The particle entanglement with position space measured by von-Neumann entropy [21] is also used to discuss the Q-C transition dynamics, where

$$S^{\rho_c}(t) = \mathrm{Tr}[\rho_c(t)\log_2\{\rho_c(t)\}], \tag{10}$$

with $\rho_c(t) = \mathrm{Tr}[\rho(t)]$ is reduced state of a particle (coin). For the DTQW system, the overall entropy in the combined (joint) subsystem of coin and position is less than the sum of the entropy for the individual subsystems. Entropy quantifies the amount of information present in a system and the correlations between quantum systems. When the Q-C transition takes place, the entanglement and quantum correlation established between the coin and position diminish. Another related measure is quantum discord. Quantum discord is a type of quantum correlation, where one can distinguish the quantum correlation over the classical correlation by finding the difference between the total correlation given by quantum mutual information $\mathcal{I}(A:B)$ and classical correlation $\mathcal{J}(B|A)$. The quantum discord of state ρ_{AB} under measurement $\{E_a\}$ is defined as [22]:

$$D(B|A) \equiv \mathcal{I}(A:B) - \mathcal{J}(B|A) \tag{11}$$

$$D(B|A) = \min_{\{\mathrm{E_a}\}} \sum_{a} p_a S\left(\rho_{B|a}\right) + S(\rho_A) - S(\rho_{AB}),$$

The non-zero discord implies the existence of non-classicality of correlation. For discords to be non-zero, the total correlation between the joint systems of $\mathcal{I}(A:B)$ exceeds the correlation of individual subsystems of ρ_A with a correlation $Corr(A,B) \leq 2$ that implies the super-correlated quantum systems. The range of correlation values of the quantum state exceeds the classical counterpart because of the existence of the hidden variable quantum system. Two approaches can be used in defining the measure of non-classicality of quantum state [23] namely trace distance scheme [24], which distinguishes certain set *C* of states by minimizing a distance, e.g. Hilbert-Schmidt distance and fidelity. This describes the extent of a given mixed state is close to the manifold of coherent states. The second approach is via the generalized (Cahil) phase-space representation of R_τ of a pure state [25], which interpolates between the Husimi (Q), the Wigner (W), and the Glauber–Sudarshan (P) representations. One can also use fidelity measure to characterize the Q-C transition, namely using

$$F(\rho_{in}, \rho_{out}) = \mathrm{Tr}\left(\sqrt{{\rho_{in}}^{1/2}\rho_{out}{\rho_{in}}^{1/2}}\right) \tag{12}$$

when $F = 0$, the ρ_{in} and ρ_{out} have orthogonal support and $F = 1$ corresponding to $\rho_{in} = \rho_{out}$ [20,26]. The off-diagonal density via

$$\mathrm{I}^{\rho_c}(\mathrm{t}) = \sum_{\mathrm{i}\neq\mathrm{j}} |\rho_c^{\mathrm{ij}}(\mathrm{t})| \tag{13}$$

with the reduced coin density matrix $\rho_c = \mathrm{Tr}_x(\rho) = \sum_x \langle x||\Psi_t\rangle\langle\Psi_t||x\rangle$ of the non-vanishing off-diagonal matrix is also a widely used coherence measure [27]. We also mention the trace distance of the density matrix defined as

$$\mathrm{D}\big(\rho_{\mathrm{in}}(\mathrm{t}),\ \rho_{\mathrm{out}}(\mathrm{t})\big) = \frac{1}{2}\mathrm{Tr}|\rho_{\mathrm{in}}(\mathrm{t}) - \rho_{\mathrm{out}}(\mathrm{t})| \tag{14}$$

where D =0 indicates pure quantum states [20,26]. Finally, the Wigner function of

$$W(x,p) = \frac{1}{\pi\hbar}\int_{-\infty}^{+\infty} \Psi^*(x+y)\Psi(x-y)e^{2ipy/\hbar}dy \tag{15}$$

is the closest phase-space representation of the quantum state of Ψ with x and p correspond to the position and momentum, respectively. By integrating the Wigner function over momentum (position), one can recover the probability density in position (momentum) space [28, 29]. For a further overview of these features, we direct interested readers to the references [30, 31]. Wigner function is a useful measure to study the quantum to classical cross-over based on the negative volume of the phase-space, indicating the non-commutative relationship of position and momentum bounded by the uncertainty principle. The volume Wigner function was used to study the evolution of "quantumness" of DTQW in the infinite lattice by Hinarejos et al.[28, 29] by comparing the Wigner function from quantum walk to the classical random walk. The negativity volume of the Wigner function correlates with the degree of non-classicality. For instance, the higher the negativity implies the stronger entanglement between coin and position, thus the greater non-classicality of the system. To distinguish the dominating decoherence mechanisms (spin and spatial (position) in quantum walk experiment of atoms walk on the optical lattice, Alberti et al.[32] proposed the measure of coherence length by taking the antidiagonal term in the density matrix to calculate the quality of "quantumness" of QW under decoherence. They used the Wigner function to the visualize effects of decoherence in suppressing the interference between possible paths of QW.

VI. EFFECT OF DECOHERENCE (NOISE) ON THE QUANTUM SYSTEM

The on-set of classicality in the DTQW driven by the noise channel (see Table 1) is shown by the emergence of the Gaussian-like shape of the probability distribution at different decoherence levels. Multi-class walks such as pure quantum walks, quantum-like walk, semi-classical like walk, and classical-like walk can be obtained from varying levels of decoherence [19] as shown in Fig 3.

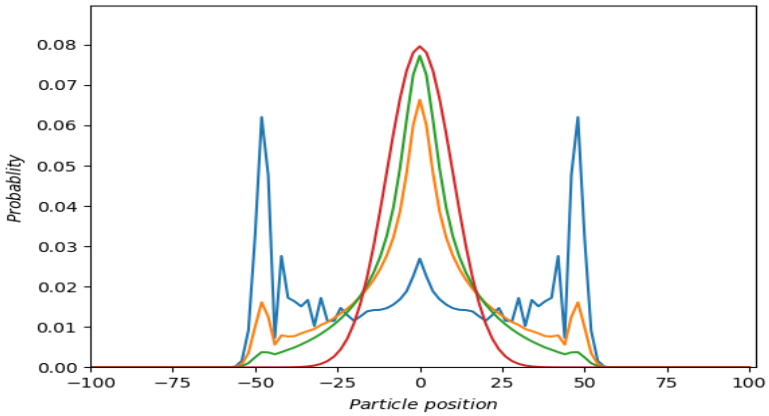

FIGURE 3. Multiclass walks produced by the varying decoherence levels in quantum walk.

The symmetries of the final probability distribution for both biased and unbiased initial states of QW remain invariant under bit-flip and phase-flip noises. It is found that the variance from the bit-flip channel (Fig. 4(a)) is uniquely independent of θ (converges to the same value) due to the randomized computational basis at maximum noise level while the variance from the phase-flip channel (Fig. 4(b)) depends on the choice of θ (non-convergence) due to asymptotic mixed state depends on θ [19, 33]. With the general amplitude noise channel as shown in Fig. 4(c), the walker exhibits the non-symmetric profile probability distribution while retaining a faster spread than a normal walk under extreme decoherence. This counterintuitive behavior is not captured by their scaling exponent of variances, but through the reduced fidelity of the walk [19]. Quantum speedup of noisy QW is also reported in [32, 33], where extreme decoherence due to a large number of coins (multi-coin) caused variance to scale quadratically because the coin space still remains "quantum". As the result, the interference effect is still persistent in coin space but not in position space.

With decoherence at the position space given by the probability of the connection between neighbor and the current position to be broken, a walker is prevented from fully undergoes complete diffusion if the link is broken too often. This walker dynamics depend on the critical decoherence value of $p_x < 0.417$ that causes the transition of QW into the super-diffusive walk (faster than classical walk) or sub-diffusion walk (slower than classical walk) [17]. As the links between neighboring sites are randomly broken with a probability p_x per unit time, the walker decohered after a characteristic time that scales as $1/p_x$[36]. The effect of the imperfect shift operations in reducing quantum features was also studied by Dur et.al [35]. The occurrence of critical decoherence value where classicality behavior emerges allows one to use noise control for DTQW. Moreover, it is found that the QW under intermediate decoherence level still possesses the "quantumness" character as the variance remains quadratic, implying that the variance is not a reliable measure of Q-C crossover.

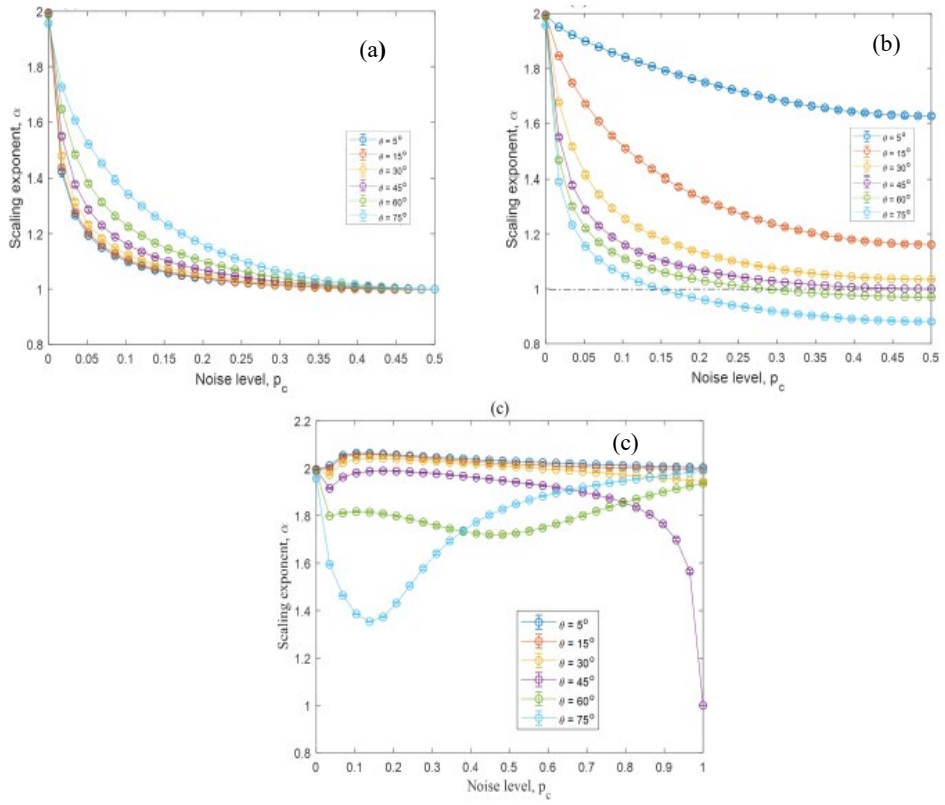

FIGURE 4. (a) The scaling exponent of the walker's variance in the presence of (a) bit-flip (BF) noise channel, (b) dephasing noise channel and (c) amplitude damping channel. The scaling exponent α is extracted from the curve of bi-logarithm variance vs step[19].

Another decoherence scheme with the time-varying strength of the coin-state measurements shows the Q-C transition inhibits the "off-on-off" model when the probability of walker to be projected at coin-state is varied over time [38]. For instance, when the probability of no measurement (projection) takes place, the QW remains as a pure quantum walk. When there is a strong probability of the walker state to be measured, the walker state reduces to the classical state. Kendon and Tregenna [39] numerically evolved the QW under decoherence due to various projections onto position space and found the optimum decoherence rate for the emergence of top-hat distribution is a function of number of steps. By applying the time-dependent shift operator with the waiting time assigned to the walker before it is allowed to move, Molfetta et al.[40] obtained another class of long memory (non-Markovian) quantum walk coined as elephant quantum walks which exhibit hyper-ballistic variance spreads over time. Interestingly, by using a non-Markovian noise channel as a source of decoherence, the walk shows the transition regime of ballistic and diffusive spread at a short time scale. While at a long time regime, the walker exhibits the fully diffusive regime with the onset of classicality measured by the disappearance of the quantum correlation [39].

The Q-C transition can be induced in the DTQW system without using any quantum noise channel by explicitly introduce sequence terms into the phase factor [40], coin parameter [41], and step [42]. Banuls.et.al [40] utilized the time-dependent phase shift parameter in the coin operator to control the Q-C transition in form of dynamical localization and quasiperiodic dynamics of DTQW 's final distribution. Following the same approach, Romanelli [45] showed by selecting

the coin time sequence, one can obtain a variety of Q-C transitions via predetermined asymptotic wave-function spreading such as ballistic, sub-ballistic, diffusive, sub-diffusive, and localized. With a single parameter step-dependent type quantum coin (SDC) [41] and position-dependent coin operator (PDC) [42] to evolve the QW density matrix, the QW exhibits multi-class walk distributions ranging from localized, classical-like, semi-classical/quantum–like, and quantum walk, which depends on the modification factor of coin parameter. Interestingly, this scheme induces crossover dynamic similar to the Anderson localization, where the mean square distance of the walker from the origin is bounded in the long-time limit due to the destructive interference on the scattering quantum path.

Similarly, one can also explicitly introduce the classical noise into the phase factor [44] or parameter [27] in the coin operator or shift operator parameter [27,45], while making the evolution "noisy" or disorder quantum walk unitary. Using disorder drawn from white noise on both coin and position, Kumar et al.[27] showed the increase of non-Markovian behavior of the walk characterized by enhancement of information backflow. To observe the influences of the disorder in the localization of the QW, Zeng and Yong [46] injected the static/dynamic phase disorder sampled from the binary/uniform distribution into the DTQW system. Both static and dynamic disorder leads to the contradictory trend on the enhanced coin entanglement when compared to the standard DTQW. It is found that the distribution of phases has minor influences on the behavior of walk. Pires and Queiros [47] introduced disorder inside the state-dependent shift operator by inducing the hopping flux probability occurring in neighbor sites via the Markov chain. Another counterintuitive trend is observed as a weak disorder via the negative correlation of binary Markov chain leads to large production of spin-lattice entanglement when compared to the case of positive correlation [47]. All the disorder schemes above induce the formation of Anderson localization, which is not sensitive to variance of the walk and can be effectively probed using inverse participation ratio (IPR) [46], coherence measure of the off-diagonal entries density matrix [46], trace distance and monitoring information backflow via Breuer, Laine, Pillo (BLP) measure [27].

The quantumness or non-classicality of QW from the Q-C transitions sometimes is not accurately captured using the trace distance scheme (e.g., variance, PDF, and trace distance) due to persistence interference in position space. To study the enhanced interference mechanisms as the ingredients of quantumness, Lopez & Paz [49] used generalized (Cahil) phase-space representation to represent the quantum states evolution as it coupled with the environment. The decoherence mechanisms in inducing Q-C transition are captured by the negative region of quasi-probability of Wigner distribution in the position-momentum space. They showed that the decoherence is inadequate to fully induce the complete transition to classicality due to the preferred observable selected by the environment is the momentum of the walker. In summary, the standard DTQW undergoes ballistic spread with the fast-reaching probability distribution in the position space. Decoherence and disorder can either reduce the speed of quantum walk into a diffusive regime or retain the quantum speedup, depending on the nature of decoherence. Both decoherence and disorder can induce localization phenomena which can be probed using the quantumness measure.

VII. CONCLUSION

We have presented a brief review of the main ideas of DTQW and the effects of decoherence from noise and disorder in triggering the Q-C transition of QW. The maximum decoherence causes the QW to fully transit to the classicality with localization in position space, while maximum disorder causes the walker to undergo Anderson localization. We noted that localizations cannot

be efficiently characterized by merely using the variance as the dynamics retain some features of the quantum speedup.

ACKNOWLEDGEMENT

This work is supported by the Malaysian Ministry of Higher Education Fundamental Research Grant Scheme (FRGS/1/2020/STG07/UM/01/2).

REFERENCES

1. J. Kempe, *Contemp. Phys* **44**, 307–327 (2003).

2. D. Aharonov, A. Ambainis, J. Kempe, and U. Vazirani, in *Proc. 33rd Annu. ACM STOC. ACM, NY* (2001), pp. 50–59.

3. A.D. Verga, *Phys. Rev. E* **99**, 1-17 (2019).

4. C.P. Williams, *Texts in Computer Science: Explorations in Quantum Computing*, Springer-Verlag, London, 2011, pp 3-49.

5. M. Mohseni, P. Rebentrost, S. Lloyd, and A. Aspuru-Guzik, *J. Chem. Phys*. **129**, 1-9 (2008).

6. A. A. Abbott and C.S. Calude, *Electron. Proc. Theor. Comput. Sci* **26**, 1-12 (2010).

7. A. M. Childs and J. Goldstone, *Phys. Rev. A* **70**, 022314 (2004).

8. V. Kendon, *Math. Struct. Comp. Sci* **17**, 1169-1220 (2007).

9. S. Srikara and C. M. Chandrashekar, *Quantum Inf. Process* **19**, 1-11 (2020).

10. J. Preskill, *Quantum* **2**, 79 (2018).

11. B. Wang, T. Chen, and X. Zhang, *Laser Photonics Rev* **14**, 1-8 (2020).

12. S. Bravyi, D. Gosset, R. König, and M. Tomamichel, *Nat. Phys* **16**, 1040 (2020).

13. A. Ambainis, E. Bach, A. Nayak, A. Vishwanath, and J. Watrous, "One-dimensional quantum walks," in *Proc. Thirty-Third Annu. ACM Symp. Theory Comput.* (New York, 2001), pp. 37–49.

14. E. Farhi and S. Gutmann, *Phys. Rev. A* **58**, 915 -928 (1998).

15. C. M. Chandrashekar, R. Srikanth, and R. Laflamme, *Phys. Rev. A* **77**, 032326 (2008).

16. H. Majury, J. Boutari, E. O'Sullivan, A. Ferraro, and M. Paternostro, *EPJ Quantum Technol* **5**, 1-12 (2018).

17. M. Annabestani, S.J. Akhtarshenas, and M.R. Abolhassani, *Phys. Rev. A* **81**, 032321 (2010).

18. B. Tregenna, W. Flanagan, R. Maile, and V. Kendon, *New J. Phys* **5**, 83.1-83.19 (2003).

19. N. I. Ishak, S. V. Muniandy, and W.Y. Chong, *Phys. A* **559**, 125124 (2020).

20. M. Nielsen and I. Chuang, *Quantum Computation and Quantum Information*, Cambridge University Press, Cambridge, 2010, pp. 387- 562.

21. Y. S. Kim, J.C. Lee, O. Kwon, and Y.H. Kim, *Nat. Phys* **8**, 117 -120 (2012).

22. K. Modi, A. Brodutch, H. Cable, T. Paterek, and V. Vedral, *Rev. Mod. Phys*. **84**, 1655-1702

(2012).

23. V. V Dodonov, *J. Opt. B Quantum Semiclassical Opt* **4**, R1–R33 (2002).
24. M. Hillery, *Phys. Rev. A* **35**, 725 -732 (1987).
25. A. Kenfack and K. Zyczkowski, *J. Opt. B Quantum Semiclassical Opt* **6**, 396–404 (2004).
26. J. Preskill, *Lecture Notes for Physics 229: Quantum Information and Computation*, Unpublished, 1998.
27. N. P. Kumar, S. Banerjee, and C.M. Chandrashekar, *Sci. Rep* **8**, 8801 (2018).
28. M. Hinarejos, M.C. Banuls, and A. Perez, *J. Comput. Theor. Nanosci* **10**, 1626-1633 (2013).
29. M. Hinarejos, M.C. Bañuls, and A. Pérez, *New J. Phys* **17**, 0-16 (2015).
30. M. Hillery, R. F. O'Connell, M. O. Scully, and E. P. Wigner, *Phys. Rep* **106**, 121–167 (1984).
31. Wolfgang P. Schleich, *Quantum Optics in Phase Spase*. WILEY-VCH Verlag, 2001.
32. A. Alberti, W. Alt, R. Werner, and D. Meschede, *New J. Phys* **16**, 123052 (2014).
33. C. M. Chandrashekar, R. Srikanth, and S. Banerjee, *Phys. Rev. A* **76**, 022316 (2007).
34. T. A. Brun, H.A. Carteret, A. Ambainis, and E. Drive, *Phys. Rev* A **67**, 1-36 (2002).
35. T. A. Brun and A. Ambainis, *Phys. Rev. Lett* **91**, 130602. (2003).
36. A. Romanelli, R. Siri, G. Abal, and A. Auyuanet, *Phys. A* **347**, 1-18 (2005).
37. H. J. Dur, W., Raussendorf, R., Kendon, V. M. and Briegel, *Phys. Rev. A* **66**, 052319 (2002).
38. P. Xue and B.C. Sanders, *Phys. Rev. A* **87**, 1-7 (2013).
39. V. Kendon and B. Tregenna, *Phys. Rev. A* **67**, 042315 (2003).
40. G. Di Molfetta, D.O. Soares-Pinto, and S.M.D. Queirós, *Phys. Rev. A* **97**, 062112. (2018).
41. P. Xue and Y. Zhang, *Chinese J. Phys* **22**, 1 -12 (2012).
42. M. C. Bañuls, C. Navarrete, A. Pérez, E. Roldán, and J.C. Soriano, *Phys. Rev. A* **73**, 1-9 (2006).
43. S. Panahiyan and S. Fritzsche, *New J. Phys* **20**, 083028 (2018).
44. R. Ahmad, U. Sajjad, and M. Sajid, *Commun. Theor. Phys* **72**, 065101 (2020).
45. A. Romanelli, Phys*. Rev. A* **80**, 042332 (2009).
46. M. Zeng and E.H. Yong, *Sci. Rep* **7**, 1-9 (2017).
47. M. A. Pires and S.M. Duarte Queirós*, Sci. Rep* **11**, 1-11 (2021).
48. S. Singh and C.M. Chandrashekar, arXiv:1711.06217v3 [quant-ph] (2020)
49. C. C. López and J.P. Paz, *Phys. Rev. A* **68**, 052305 (2003).